Available online at www.sciencedirect.com
ScienceDirect
Tetrahedron
Tetrahedron 63 (2007) 6915–6923

Synthesis and NMR characterization of *cis* and *trans* decahydro-2a,4a,6a,8a-tetraazacyclopent[*fg*]acenaphthylene. Solid state structure of the trans stereoisomer. Modelling studies

Maria Argese,[a,*] Marino Brocchetta,[a] Mario De Miranda,[a] Andrea Ferraris,[a] Paolo Dapporto,[b] Paola Paoli[b] and Patrizia Rossi[b]

[a]*Milano Research Centre, Bracco Imaging spa, via E. Folli 50, 20134 Milano, Italy*
[b]*Dipartimento di Energetica 'Sergio Stecco', Università di Firenze, via S. Marta 3, 50139 Firenze, Italy*

Received 15 December 2006; revised 26 March 2007; accepted 12 April 2007
Available online 19 April 2007

Abstract—The reduction with Vitride® of the cis and trans isomers of octahydro-2a,4a,6a,8a-tetraazacyclopenten[*fg*]acenaphthylene 1,2-diones (**5** and **6**) and octahydro-2a,4a,6a,8a-tetraazacyclopenten[*fg*]acenaphthylene 3,4-diones (**7** and **8**) led to the *cis* **9** and the so far unknown *trans* **10** isomers of decahydro-2a,4a,6a,8a-tetraazacyclopent[*fg*]acenaphthylene. The stereochemistry of **9** and **10** was determined by comparison of the NMR coupling constants of the proton signals of the ethinic bridge. The results were confirmed by the solid state structure of the trans isomer (**10**) determined by single crystal X-ray diffraction. Given that the *trans* bis-aminal species **2** and **4** can undergo rearrangement, i.e. stereoisomerization into the corresponding cis ones (**1** and **3**, respectively), the conformational behaviour of species **1**–**4** was investigated by means of both molecular mechanics (MM) and quantum chemical (QC) approaches. The theoretical study was completed by including diamides **5**–**8** and the final products **9** and **10**.

1. Introduction

In a recent article,[1] as well as in a previous patent,[2] we reported that, by amidation of a mixture containing the bis-aminals **1**–**4** with diethyl oxalate (DEO) in EtOH at reflux, the related mixture containing *cis* octahydro-2a,4a,6a,8a-tetraazacyclopent[*fg*]acenaphthylene 1,2-dione (**5**) and *cis* octahydro-2a,4a,6a,8a-tetraazacyclopent[*fg*]acenaphthylene 3,4-dione (**7**) is obtained (Scheme 1). The result is a consequence of a rearrangement, which transforms **2** and **4** into **1** and **3**, respectively, before the amidation.[1,3] Accordingly, the trans isomers **6** (*trans* octahydro-2a,4a,6a,8a-tetraazacyclopent[*fg*]acenaphthylene 1,2-dione) and **8** (*trans* octahydro-2a,4a,6a,8a-tetraazacyclopent[*fg*]acenaphthylene 3,4-dione) are not formed. In the presence of 2-pyridinol also, the trans compounds are absent, but when the reaction is catalyzed with MeONa, the amidation becomes faster than the stereoisomerization, and along with **5** and **7**, compounds **6** and **8** are also obtained.[1] The latter, after reduction of the amide carbonyls, could obviously disclose route to **10**, a compound not yet reported in the literature.[4] Such a synthetic strategy has never been used in the past, as compounds **6** and **8** were unknown.

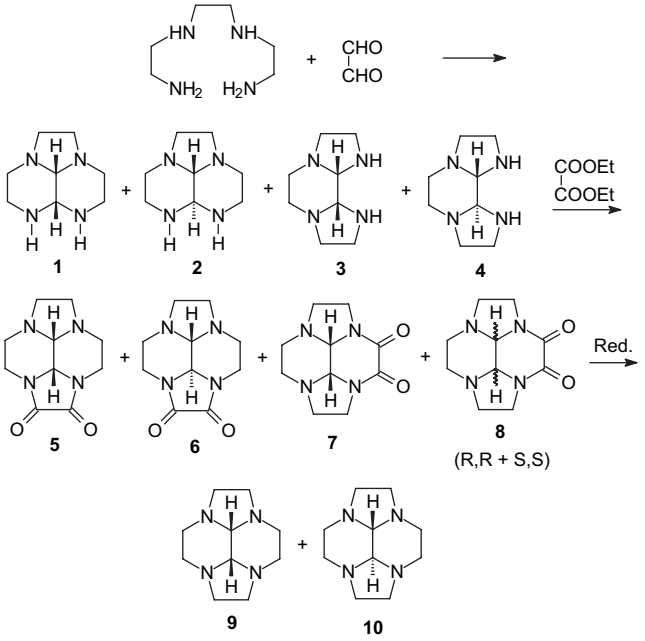

Scheme 1.

2. Results and discussion

The reduction with Vitride®,[7] of the amide carbonyls of a mixture containing the cis isomers **5** and **7**[1] led to a product,

* Corresponding author. E-mail: maria.argese@poste.it

0040–4020/$ - see front matter © 2007 Elsevier Ltd. All rights reserved.
doi:10.1016/j.tet.2007.04.036

which was recovered in good yield by a quite simple procedure. We were confident that this compound corresponded to *cis* decahydro-2a,4a,6a,8a-tetraazacyclopent[*fg*]acenaphthylene (**9**). Analogously, we could use either one of the previously prepared trans isomers **6** or **8**[1] for the synthesis of the *trans* tetracycle, but due to the low quantity of these product at disposal, we decided to reduce a mixture containing **5**–**8**, which could be easily prepared.[1] The subsequent chromatographic separation of the reduced mixture afforded, apart from **9**, a new compound having the same mass of **9** but different mp, TLC R_f and GC retention time. To this product we tentatively assigned the structure of *trans* decahydro-2a,4a,6a,8a-tetraazacyclopent[*fg*]acenaphthylene (**10**).

Taking advantage of the NMR experience acquired with compounds **5**–**8**, whose stereochemistry was known by single crystal X-ray diffraction,[1,3] we could attribute the correct stereochemistry to **9** and **10**, even before the solid state structure determination of **10** by X-ray diffraction. Indeed, the discrimination between cis and trans isomers was achieved by the analysis of the coupling constants (*J*) of the proton signals of the ethinic bridge. The latter showed a doublet multiplicity for compounds **5** and **6** and the *J* values could be easily deduced, while for the symmetric compounds **7** and **8** the C*H* signals were singlets. Accordingly, the direct calculation of *J* was prevented, but as it is known that the analysis can also be performed on the signals of rare isotope satellites,[8] we turned our attention to the ^{13}C satellite analysis of the ^{1}H NMR signals. The presence of a ^{13}C atom in only one of the halves produces a loss of molecular symmetry, which enables the determination of the coupling constant between otherwise equivalent protons (Figs. 1 and 2). The *J* values of the cis compounds **5** and **7** resulted lower than those of the related trans isomers **6** and **8** (Table 1). This is in agreement with the theory,[9] which correlates the vicinal proton coupling constant to the dihedral angle. The latter,

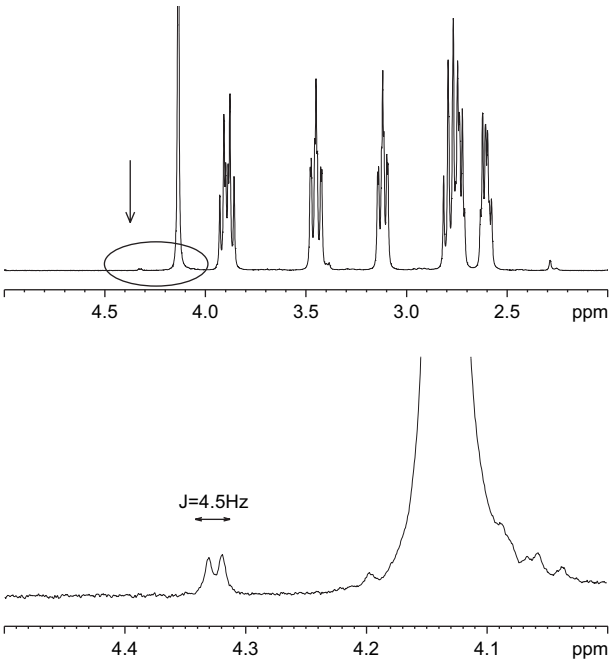

Figure 1. *J* value for the ethinic protons of **7**.

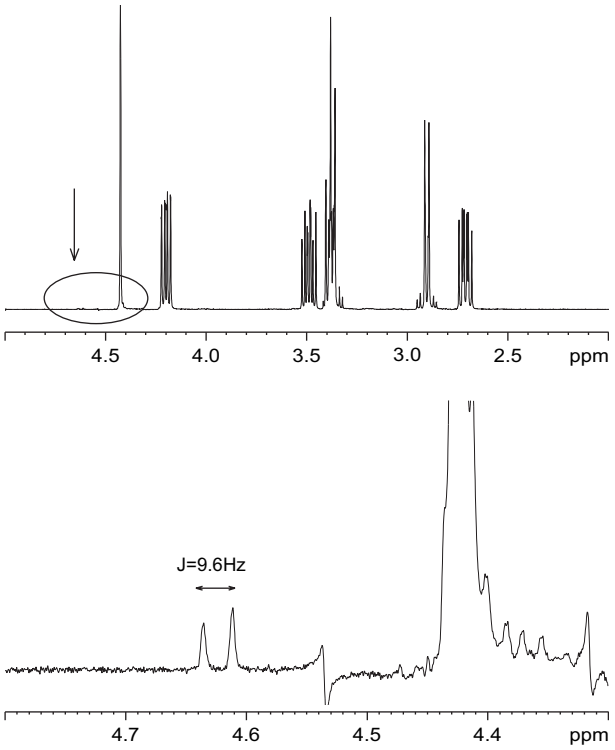

Figure 2. *J* value for the ethinic protons of **8**.

although not the only one, is the most important factor affecting the *J* values. Reliable results in structural analysis are to be expected from the comparison of closely related species, as in our case in which a large coupling constant is associated with the trans structure with a dihedral angle close to 180°, while a small one with a cis structure with a dihedral angle in the 40° range.

The same study allowed us to obtain the coupling constant of **9** (Fig. 3), while for compound **10** the ^{13}C satellites of the C*H* signals unfortunately overlapped the CH_2 signals. Accordingly, a ^{1}H–^{13}C reverse HSQC 2D experiment was performed using the INVIEAGSSI pulse program from Bruker library and removing the GARP decoupling during acquisition so that the cross-peaks between carbon and proton resulted in correspondence with the ^{13}C satellites in the proton spectrum (f2 dimension). The experiment gave a phase sensitive spectrum, which was properly phased using the 2D Bruker phase routine and a resolution sufficient to show that the multiplicity pattern was obtained using the following parameters: fid resolution=78.6 Hz (f1)/0.1 Hz (f2); matrix size=128 (f1)×8192 (f2). Extracting the row of the desired cross-peak from the 2D spectrum, it was possible to obtain the *J* value for **10**, which resulted in the range of the trans isomers (Fig. 4) (Table 1). In order to verify the appropriateness of the method, the same experiment with the same parameters was run for compound **9**. The *J* value

Table 1. *J* values (Hz) found for the proton signals of the ethinic bridge of compounds **5**–**10**

5	**6**	**7**	**8**	**9**	**10**
4.6	6.2	4.5	9.6	3.0	9.2

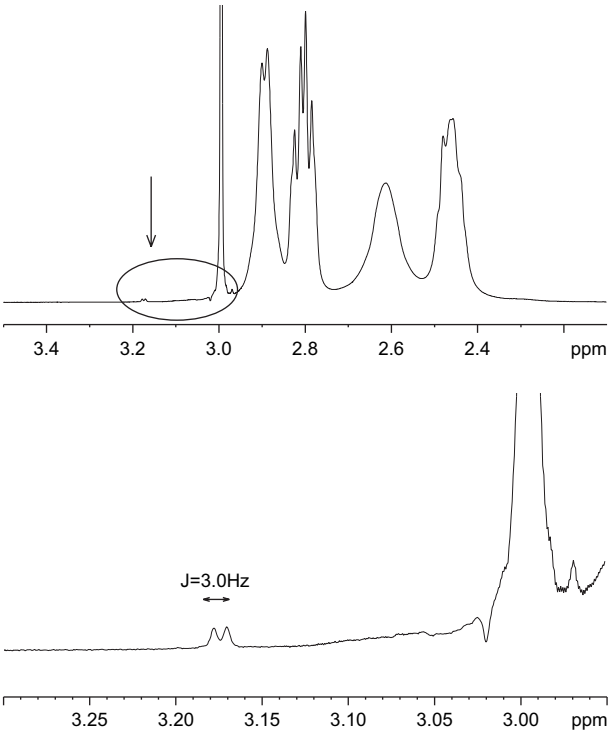

Figure 3. *J* value for the ethinic protons of **9**.

obtained from the 2D method (3.1 Hz) (Fig. 5) resulted very close to the one (3.0 Hz) obtained with the direct measurement in the 1D spectrum and was related to a cis compound.

The further and definitive proof of the stereochemistry of **10** was achieved when we finally obtained crystals suitable for the solid state structure determination by X-ray diffraction.

Figure 6 shows an ORTEP3 view of compound **10**, which is in the asymmetric unit and interacts via a network of weak hydrogen bonds[10] with its symmetry related images (see

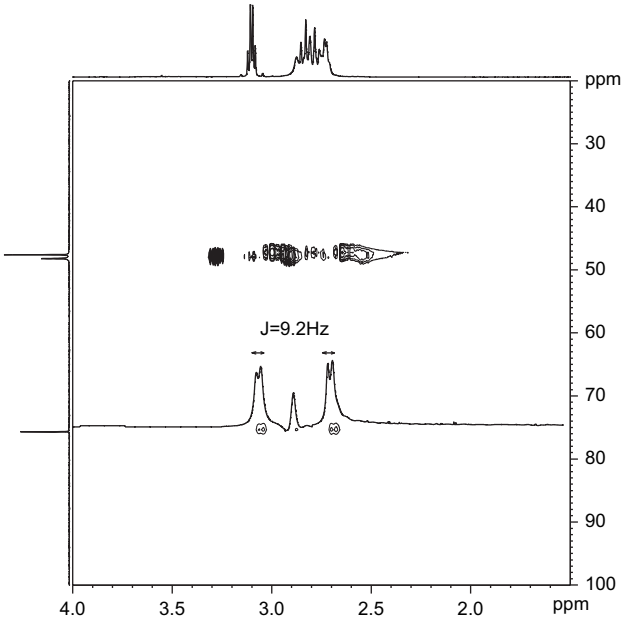

Figure 4. *J* value for the ethinic protons of **10**.

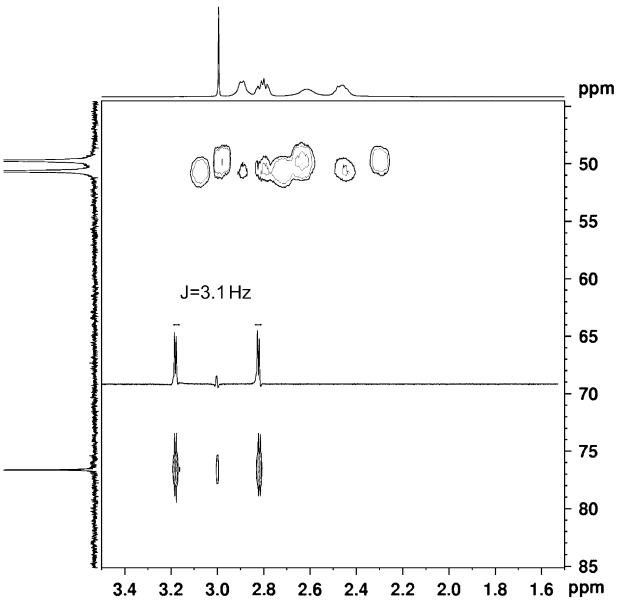

Figure 5. *J* value for the ethinic protons of **9** (from the 2D experiment).

Table 2). Table 3 lists experimental (X-ray data) and calculated (quantum chemical) bond distances.

Both the six- and five-membered rings show their usual conformation, that is, chair and envelope, respectively. The position, i.e. axial (A) or equatorial (E) of the bound $-CH_2$ groups belonging to the five-membered ring results in the EAAE isomer (see Section 4.4.1).

The analysis of the experimental bond distances (Table 3) reveals that the CH–CH bond ($d1$=1.496(2) Å) is by far shorter than the CH_2–CH_2 ones ($d2$, mean value 1.54 Å).

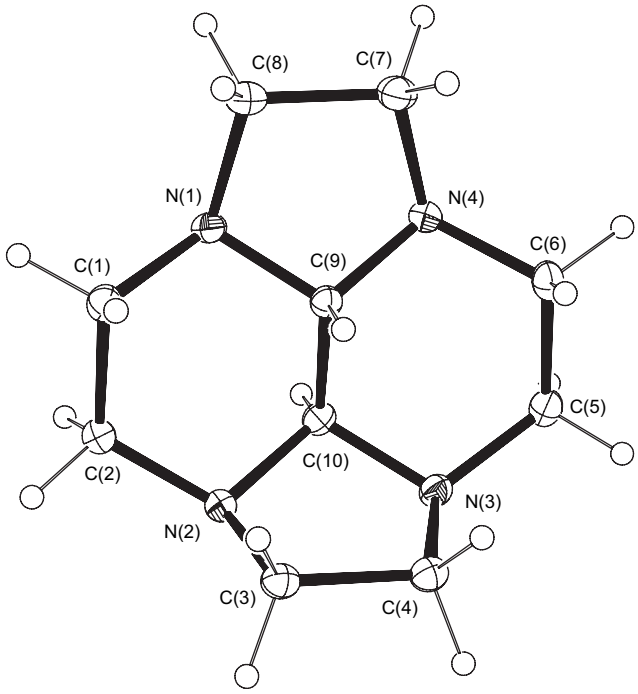

Figure 6. ORTEP3 view of compound **10**. (Thermal ellipsoids are set to 30% probability).

Table 2. Intermolecular contacts found in the crystal lattice of **10**

Donor–H···acceptor	Donor···acceptor distance (Å)	H···acceptor distance (Å)	Donor–H··· acceptor angle (°)
C(1)–H(1a)···N(3)[a]	3.817(2)	2.83(2)	168(1)
C(2)–H(2b)···N(4)[b]	3.957(2)	2.98(2)	162(1)
C(7)–H(7a)···N(2)[c]	3.583(2)	2.89(2)	126(1)
C(8)–H(8a)···N(2)[c]	3.490(3)	2.69(2)	135(1)
C(4)–H(4a)···N(3)[d]	3.711(3)	2.97(2)	131(1)
C(3)–H(3a)···N(3)[d]	3.651(2)	2.89(2)	133(1)
C(4)–H(4a)···N(2)[d]	3.792(3)	2.82(2)	163(1)
C(5)–H(5a)···N(1)[e]	3.455(2)	2.53(2)	162(1)

[a] $=x+1/2, -y+1/2, z+1/2$.
[b] $=x+1, y, z$.
[c] $=x-1/2, -y+1/2, z+1/2$.
[d] $=-x+1, -y+1, -z$.
[e] $=-x+1/2, y+1/2, -z+1/2$.

The opposite, i.e. $d1>d2$, holds in fragments featuring a 1,4,5,8-tetraazadecalin (TAD) core[11] retrieved in the Cambridge Structural Database.[12] The CH–N bonds are shorter than the CH_2–N ones, a trend particularly significant for the bonds about N(1) and N(4), which, as a whole, appear shorter than those about the corresponding N(2) and N(3) atoms. The equivalent couples N(1)/N(4) and N(2)/N(3) differ from the positions of their lone pair and, correspondingly, of the $-CH_2$ grouping of the five-membered ring: axial–equatorial (A–E), respectively, on the first couple; equatorial–axial (E–A), respectively, on the latter.

Maybe stereoelectronic effects, such as the anomeric one,[13] could explain such structural features, which are maintained also in the HF and DFT optimized molecule (see Table 3).

In order to find a rationale for these structural differences featuring the nitrogen atoms N(1)/N(4) and N(2)/N(3), a natural bond analysis (NBO) was performed on the HF optimized molecule. Actually, the lone pairs on the nitrogen atoms are interested in hyper-conjugative $n(N)\rightarrow\sigma^*(C–Y)$ interactions mainly within the six-membered rings. In fact, the lone pairs on N(1) and N(4) are aligned in an antiperiplanar geometry and interact with the axial C–H bonds of C(1), C(6) and C(9), while those on N(2) and N(3) have the correct orientation to conjugate with the σ* C(1)–C(2), C(5)–C(6) and C(9)–C(10) bonds. The estimation of the relative energetic importance of these hyper-conjugative effects suggests that while the axial lone pairs on N(1)/N(4) interact mainly with the σ*C(9)–H [vs the C(1)–H, C(6)–H], the equatorial lone pairs on N(2)/N(3) conjugate preferentially with the σ* C(1)–C(2) and C(5)–C(6) [vs C(9)–C(10)]. It is noteworthy that in the optimized *trans* tetraazadecalin isomers (EEEE, AAAA and EAAE) the different $n(N)\rightarrow\sigma^*(C–Y)$ interactions are energetically equivalent and, accordingly, no significant differences affect the C–N and C–C bond distances (mean values 1.45 and 1.53 Å, respectively). The comparison of the results of NBO analyses on optimized 2EAAE and 2AEEA isomers (see Scheme 2) suggests that it is the CH_2–CH_2 bridge in equatorial position, which causes the asymmetry in the conjugation effects and, as a consequence, in the geometry. In fact in the 2AEEA species the hyper-conjugative interactions, as well as the C–N and C–C bond distances are all comparable. On the contrary in the 2EAAE isomer there are energetic and geometrical differences, a trend is consistent with that observed in **10**. A further support to the importance of the equatorial position of the CH_2–CH_2 bridge in determining an asymmetry in the tricyclic molecule was obtained from an ab initio optimization of two different isomers of dodecahydroacenaphthylene: the AA and EE ones (the acronyms refer to the position of the $-CH_2$ groupings of the five-membered ring with respect to the tertiary carbon atoms). In the AA isomer the CH–CH and CH_2–CH_2 are almost identical, while in the molecule bearing an 'equatorial' five-membered ring we observed the same trend found in **10**.

Table 3. Selected bond distances (Å) for **10** as obtained from X-ray diffraction and modelling studies

	X-ray diffraction	HF/6-31G** (full opt)	B3LYP/6-31G** (full opt)
N(1)–C(1)	1.463(2)	1.450	1.461
N(1)–C(8)	1.476(3)	1.460	1.474
N(1)–C(9)	1.438(2)	1.425	1.439
N(2)–C(2)	1.475(2)	1.460	1.471
N(2)–C(3)	1.480(2)	1.461	1.476
N(2)–C(10)	1.459(2)	1.441	1.456
N(3)–C(4)	1.485(2)	1.461	1.476
N(3)–C(5)	1.473(3)	1.460	1.471
N(3)–C(10)	1.458(2)	1.441	1.456
N(4)–C(6)	1.465(2)	1.450	1.461
N(4)–C(7)	1.478(2)	1.460	1.474
N(4)–C(9)	1.438(2)	1.425	1.439
C(1)–C(2)	1.544(3)	1.549	1.559
C(3)–C(4)	1.541(3)	1.550	1.557
C(5)–C(6)	1.541(3)	1.549	1.559
C(7)–C(8)	1.552(3)	1.560	1.568
C(9)–C(10)	1.496(2)	1.501	1.513

Given that the *trans* bis-aminals species **2** and **4** (Scheme 1) can undergo rearrangement, i.e. stereoisomerization into the corresponding cis ones (**1** and **3**, respectively) and that, to the best of our knowledge, only one tricyclic species has been characterized in the solid state[14] (it shows a cis-junction between the six-membered rings), we decided to investigate the energetic and the conformational behaviour of species **1**–**4** by means of both molecular mechanics (MM) and quantum mechanics (QM) approaches. The theoretical study was completed also by including diamides **5**–**8** and the final products **9** and **10**.

A bibliographic search revealed that the conformational behaviour of TAD, together with some derivatives, has been investigated by means of NMR and MM.[15] Its intramolecular dynamics can be rationalized according to the following types of motion: trans–cis isomerization (by means of aminal ring-chain tautomerism), ring inversion (in cis isomers only) and nitrogen inversion. The X-ray structure of the trans-fused species has also been reported.[16] Obviously, molecules **1**–**10** can undergo less significant conformational changes with respect to TAD, given the constraints imposed by the five-membered ring/ring closure. However, steric interactions of *peri*-substituents, lone pair–lone pair, n_π–σ* interactions (as already pointed out) and NH···N hydrogen bonds are still active, although not in all the molecules, and should influence their dynamics as well as their solid state 3D arrangement.

Molecular dynamics in vacuum showed that the conformational space accessible for **1**–**10** is quite limited as provided

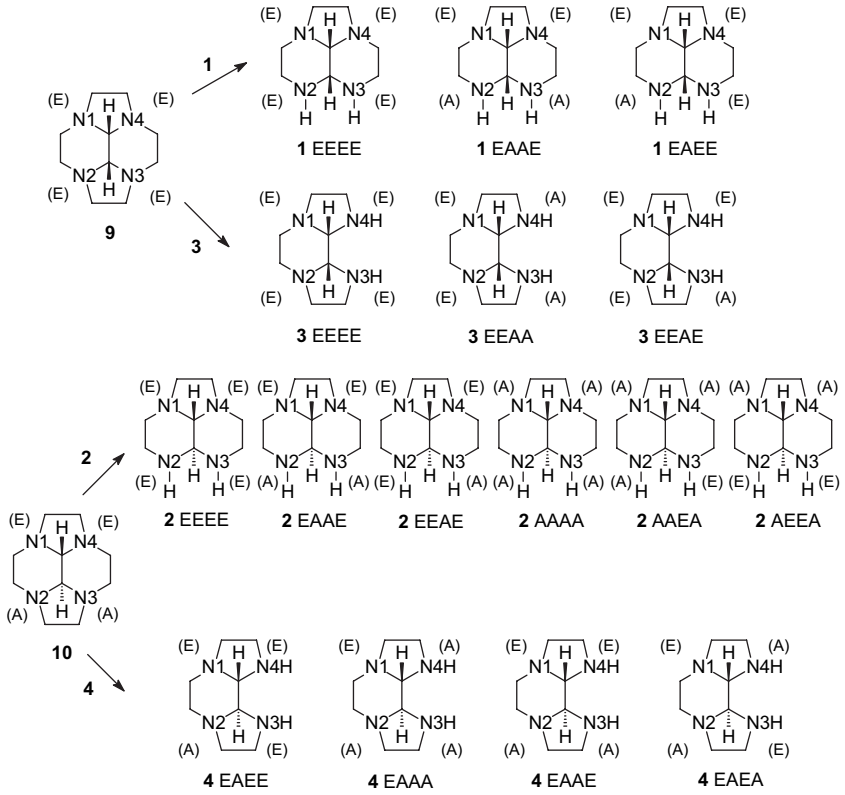

Scheme 2. Different isomers of the tricyclic intermediates **1**–**4** were generated according to the procedure in Section 4.4.1 (i). Letters (A/E) refer to the conformations on N atoms.

by the rather small number of conformers spotted during the simulations. As expected on the basis of their stereochemistry (sp^2 hybridized nitrogen atoms) diamides **5**–**8** appear as the most constrained: molecule **6** results the most rigid (only two different conformers were classified, rms deviation 0.45 Å). On the contrary molecule **1** shows the largest variability: 11 different conformers were found (max rms deviation 0.67 Å) differing up to 12 kcal mol^{-1}. As a general trend, cis-fused isomers appear more flexible than the corresponding trans one. In most cases, the different conformers recognized can be ascribed to nitrogen inversion and, more rarely, to ring inversion processes. With some exception (**3** and **4**), cis-fused molecules appear more stable than the corresponding trans ones.

Monte Carlo conformational searches, including the effect of the solvent (water) carried out for all compounds, showed a similar behaviour, with the cis-fused isomers more flexible than the trans-fused ones. Again, considering the filtering conditions reported in the Section 4, molecule **6** appeared the most rigid (1 conformer selected) and molecule **1** the most flexible (30 conformers). From an energetic point of view, all the cis-fused molecules were more stable than the corresponding trans ones. In all cases, HF geometry optimizations did not produce any relevant change in the 3D arrangement of the molecules with respect to their starting geometry. The most stable isomer (Table 4) of each tricyclic intermediate (**1**–**4**) has the two hydrogen atoms bound to the secondary nitrogens in an A/E disposition, thus optimizing

Table 4. Energy differences (cis/trans couples relative energies, kcal mol^{-1}) for the intermediates and the final compounds as obtained from quantum chemical calculations

Compound[a,b]	Relative energy HF/6-31G** (full opt)	Relative energy MP2/6-31G**//HF/6-31G**	Relative energy B3LYP/6-31G** (full opt)	Relative energy MP2/6-31G**//B3LYP/6-31G**
1	0.00	0.00	0.00	0.00
2	1.62	2.98	1.40	1.52
3	0.00	0.00	0.00	1.43
4	1.14	3.24	0.61	0.00
5	0.00	0.34	1.15	0.00
6	0.41	0.00	0.00	0.46
7	0.00	0.00	0.00	0.00
8	1.17	2.65	1.22	1.12
9	0.00	0.00	0.00	0.00
10	6.53	7.00	5.71	6.51

[a] For the compounds **1**–**4** and **9** the most stable conformers obtained from modelling (details in Section 4.4.1) were: EAEE (**1**); EEAE (**2**); EEAE (**3**); EAEA (HF optimization) and EEEE (DFT optimization) (**4**) and EEEE (**9**).

[b] For compounds **5**–**8**[1,3] and **10** (Fig. 5) the data are referred to the conformations deduced by X-ray diffraction analysis.

their relative distance as well as that separating the nitrogen lone pairs, hence the non-bonding interactions.

At DFT level all the minima were equivalent to the HF ones, with one exception: the most stable conformer for the compound **4** differed for N2 and N4 inversions, corresponding to the EEEE isomer. However, the E/E disposition of the hydrogen atoms bound to secondary nitrogens guaranteed their relative maximum distance, as well as one of the respective lone pairs.

In general, QC results (Table 4) confirm the MM trend, i.e. cis-fused products appear lower in energy than the corresponding trans ones as already found for TAD.[15] Since this tendency is less significant for the **3** and **4** couples (no TAD core) and it is definitely dubious for the **5** and **6** ones (where the TAD core is somewhat perturbed by the presence of sp^2 atoms in the five-membered cycle),[1] perhaps the cis-versus trans-junction preference is an intrinsic feature of the TAD core.

3. Conclusion

A new synthetic strategy, starting from diones **5**–**8**, allowed us to synthesize compound **9** and the so far unknown compound **10**, whose stereochemistry was assigned by solid state X-ray diffraction.

The analysis of the NMR coupling constants for the hydrogens of the ethinic bridge afforded an independent tool for the attribution of the stereochemistry to compounds **5**–**10**.

In the solid state structure, **10** shows an EAAE conformation on the nitrogen atoms. The shortening of the CH–CH bond distance, with respect to the CH_2–CH_2 was ascribed to the equatorial position of the CH_2–CH_2 bridge of the five-membered ring (NBO analysis on the ab initio optimized molecule). The conformational space accessible to molecules **1**–**10** is quite limited both in vacuum and in solvent (water), diamides **5**–**8** being the most constrained. As a general trend, cis-junctions are associated with a larger conformational freedom and a greater energy stability with respect to the trans ones. The TAD core on its own could account for the latter energetic trend.

4. Experimental

4.1. General

All reagents and solvents, obtained from commercial sources, were used without further purification. Melting points (°C, uncorrected) were measured with a Büchi 510 instrument. TLC was carried out on 60 F_{254} silica gel plates using $CHCl_3$/CH_3OH/25% NH_4OH, 6/3/1 as the eluent and iodine vapours for the visualization. GC analyses were performed with a Hewlett–Packard HP 5890 instrument using: CP Sil 19 CB column (25 m×0.32 mm; film thickness 0.2 mm); He pressure 20 psi; injector and detector (FID) temperatures 250 and 275 °C, respectively; oven temperature timetable as follows: first isotherm at 120 °C for 5 min; 15 °C/min ramp to 260 °C; second isotherm at 260 °C for 12 min; injection (1 μL) of a 20 mg/mL solution in toluene containing acenaphthene (10 mg/mL) as an internal standard. IR spectra were recorded on a Perkin–Elmer 882 spectrophotometer, using potassium bromide disks. MS spectra were acquired on a TSQ700 ThermoFinnigan Spectrometer using CH_3OH as the solvent. ^1H and ^{13}C NMR spectra were recorded at 298 K in D_2O at 400.13 and 100.61 MHz, respectively, with a Bruker DRX 400 spectrometer. In order to have a complete assignment of the structures, 2D spectra were recorded using ^1H–^1H COSY45, HMQC and HMBC standard pulse sequences. The chemical shifts are given in δ units (ppm) relative to TMS (δ=0). Elemental analyses were carried out at the Redox Laboratories (Monza, Milano, Italy).

4.2. Synthetic methods

4.2.1. *cis* Decahydro-2a,4a,6a,8a-tetraazacyclopent[*fg*]-acenaphthylene (9). A mixture containing **5** and **7** in about 2/1 ratio[1] (10.0 g; 0.045 mol) was added to a 70% toluene solution of Vitride®,[7] (50.4 g; 0.174 mol) diluted with toluene (100 mL) and stirred at 40 °C under a nitrogen atmosphere. In about 10 min the suspension was heated to 112 °C and turned into a clear solution. After 1 h in the same conditions, when the conversion (GC) reached 97%, the mixture was cooled to rt and 5% aq NaOH (29 mL) was cautiously added dropwise. The two phases were separated and the viscous aqueous phase was extracted with toluene (2×25+50 mL) then the combined organic phases were evaporated to a residue. The latter was dissolved in water (40 mL) and the solution was loaded onto a strong cation exchange resin (Amberlite Amberjet®, 80 mL) column, which was eluted with water to neutrality. The subsequent percolation of 2.5% NH_4OH (450 mL) afforded a basic eluate, which was evaporated to dryness. The residue was extracted with hexane (90 mL) and the organic phase was evaporated to afford **9** (7.1 g; 84%). Mp 90–92 °C.[17] TLC R_f 0.8; GC 100% (rt 8.5 min); IR (KBr) ν 2938, 1465 cm^{-1}; ^1H NMR (400 MHz, D_2O) δ 2.46 (m, 4H: CH_2), 2.61 (br m, 4H: CH_2), 2.80 (m, 4H: CH_2), 2.89 (m, 4H: CH_2), 2.99 (s, 2H: C*H*); ^{13}C NMR (100 MHz, D_2O) δ 49.7 (*C*H_2), 50.6 (*C*H_2), 76.6 (*C*H); MS *m*/*z* (ESI) 195 $(M+H)^+$, 217 $(M+Na)^+$; Anal. Calcd for $C_{10}H_{18}N_4$: C, 61.82; H, 9.34; N, 28.84. Found: C, 62.02; H, 9.38; N, 29.07.

4.2.2. *trans* Decahydro-2a,4a,6a,8a-tetraazacyclopent-[*fg*]acenaphthylene (10). A mixture containing **5** (61.5%), **6** (16.4%), **7** (3.4%) and **8** (18.7%)[1] (8.0 g; 0.036 mol) was reduced under the conditions used to obtain **9**. The final residue (5.4 g containing **9** and **10** in 2.5/1 ratio,[19] as determined by GC) was subjected to silica gel chromatography ($CHCl_3$/CH_3OH 9/1) to afford **10** (0.7 g; 28%[20]). Mp 136–139 °C;[17] TLC R_f 0.54; GC 100% (rt 10.4 min); IR (KBr) ν 2940, 1484 cm^{-1}; ^1H NMR (400 MHz, D_2O) δ 2.73 (m, 4H: CH_2), 2.81 (m, 8H: CH_2), 2.87 (s, 2H: C*H*), 3.10 (m, 4H: CH_2); ^{13}C NMR (100 MHz, D_2O) δ 47.6 (*C*H_2), 48.2 (*C*H_2), 75.6 (*C*H); MS *m*/*z* (ESI) 195 $(M+H)^+$, 217 $(M+Na)^+$; Anal. Calcd for $C_{10}H_{18}N_4$: C, 61.82; H, 9.34; N, 28.84. Found: C, 61.65; H, 9.46; N, 28.65.

4.3. X-ray crystallographic study

Crystals of **10** used for X-ray diffraction analysis were grown at rt from a saturated solution in hexane. Crystals of

Table 5. Crystal data and structure refinement for **10**

Empirical formula	$C_{10}H_{18}N_4$
Formula weight	194.28
T (K)	120
λ (Å)	0.71073
Crystal system, space group	monoclinic, $P2_1/n$
Unit cell dimensions (Å, °)	a=7.6341(9); b=11.457(1), β=96.873(9); c=11.172(1)
Volume (Å^3)	970.1(2)
Z, d_{calcd} (g cm^{-3})	4, 1.330
μ(mm^{-1})	0.084
F(000)	424
Crystal size (mm)	0.4×0.5×0.55
2θ Range for data collection (°)	8.92–51.94
Reflections collected/unique	7510/1639 [R(int)=0.0446]
Refinement method	Full-matrix least-squares on F^2
Data/restraints/parameters	1639/0/199
Final R indices [$I>2\sigma(I)$]	$R1$=0.0395, $wR2$=0.0714
R indices (all data)	$R1$=0.0750, $wR2$=0.0788

9, either as free base from hexane, or as the hydrochloride salt from methanol or acetonitrile, were obtained but unfortunately, in any cases, they resulted as twinned crystals, whose structure was not solvable by single crystal X-ray diffraction. Intensity data collection for compound **10** was performed by using an Oxford Diffraction XCalibur diffractometer equipped with a CCD area detector using the radiation Mo Kα (λ=0.7107 Å). Diffraction data were collected with the CrysAlis CCD program[21] and reduced with the CrysAlis RED program.[22] Absorption correction was performed with the program ABSPACK in CrysAlis RED. Structure was then solved using the SIR97 program[23] and refined by full-matrix least squares against F^2 using all data (SHELX 97).[24] All the non-hydrogen atoms were refined anisotropically. All the hydrogen atoms were found in the Fourier difference map. Geometrical calculations were performed by PARST97[25] and molecular plots were produced by the program ORTEP3.[26]

Crystallographic data and refinement parameters are reported in Table 5.

Crystallographic data for compound **10** have been deposited with the Cambridge Structural Data Centre as supplementary publication number CCDC 628339.

4.4. Molecular modelling studies

4.4.1. General strategy. The starting geometries of molecules **5**–**8**[1,3] and **10** were those of their solid state structures. For compounds **1**–**4** and **9**, whose X-ray structural parameters were not available, starting geometries were generated using different approaches, (i) and (ii), for comparative purposes.

(i) For **1**, **3** and **9**, the atomic coordinates of the *cis* decahydro-2a,4a,6a,8a-tetraazacyclopent[*fg*]acenaphthylene-2a,6a-bis(borane)[27] (YAHTOQ refcode) backbone were used, while the input geometries of **2** and **4** were derived from that of the parent molecule **10** (Scheme 2). In principle, for the tricyclic molecules **1**–**4** several conformational isomers should be taken into account, depending on the axial or equatorial position (A or E, respectively) of the hydrogen atoms bound to the secondary nitrogen atoms (see Scheme 2). The A or E letter labelling the secondary nitrogen atoms refers to the axial (A) or equatorial (E) position of the bound hydrogen atom. For the tertiary nitrogen atoms the A or E label arises from the position of the bound –CH_2 group belonging to the five-membered ring as found in the solid state structure. In the isomers nomenclature the first letter refers to the conformation on the N(1) atom and then it proceeds counterclockwise along the fused rings.

(ii) Starting models (**1**–**4** and **9**) were obtained from Monte Carlo searches [details in Section 4.4.2 (ii)].

4.4.2. Molecular mechanics calculations. Two parallel strategies were used to explore the conformational space accessible to molecules **1**–**10** in vacuum and in solvent.

(i) Molecular dynamics (MD) simulations were performed in vacuum at 1000 K (CVFF force field) using the MSI software programs Insight II and Discover[28] (version 98.0). The Verlet leapfrog algorithm, with a time step of 1 fs, was used for integration of equations of motion in all simulations. Before starting each MD simulation, the starting models, derived as outlined in Section 4.4.1 (**5**–**8**, **10**) and 4.4.1 (i) (**1**–**4**, **9**), were optimized until the convergence criterion was met (<0.01 kcal mol^{-1} Å^{-1}). For every MD run the system was allowed to equilibrate for 10 ps and then a 1000 ps dynamic was performed. Snapshot conformations were collected for every pico second, minimized and ranked accordingly to their energy contents. Then, for each molecule, conformers, differing in energy for 1 kcal mol^{-1}, were selected and clustered in four intervals on the basis of their structural similarity.

(ii) The Monte Carlo method,[29] as implemented in Macromodel software program (version 9.0) in Maestro (version 7.0)[30] was used to perform conformational searches for all the molecules. The Amber * force field,[31] and, as an implicit solvation treatment, the GB/SA solution model[32] were employed. For each structure, a global search was performed, with a maximum number of 5000 Monte Carlo steps: the conformers were minimized by the Truncated Newton Conjugate Gradient method,[33] with a derivative convergence criterion at a value of 0.01 kcal mol^{-1} Å^{-1}; they were then filtered using an energy cut-off of 12 kcal mol^{-1} and a threshold of 0.25 Å as the maximum distance between corresponding heavy atoms after superposition.

4.4.3. Quantum chemical calculations. Parallel QC calculations, (i) and (ii), were carried out on molecules **1**–**10**.

(i) The geometry of the starting models obtained as described in Section 4.4.1 (**5**–**8** and **10**) and 4.4.1 (i) (**1**–**4** and **9**) was optimized using the GAUSSIAN 03 (Revision B.05)[34] package implemented on a personal computer.
In all cases the basis set was 6-31G(d,p).[35] The reliability of the stationary points, found by means of HF-SCF calculations and the Berny algorithm,[36] was assessed by the evaluation of the vibrational frequencies. Then single point MP2[37] calculations [6-31G(d,p), basis set] were performed on the optimized structures. NBO analyses were performed using the NBO 5.0 program.[38]

(ii) To take into account the effect of electron correlation on the molecular geometry, further calculations at DFT level were carried out on the starting models obtained from Monte Carlo method [Section 4.4.2 (ii)]. The Spartan'02[39] software on a SGI Indigo 2 IMPACT 10000 workstation was used. Gas-phase geometry optimizations were performed by the Becke's Three Parameter Hybrid functional[40] using the LYP Correlational functional[41] [B3LYP method, 6-31G(d,p) basis set]; again, a single point energy calculation at MP2 level [6-31G(d,p), basis set] was performed on each resulting structure.

References and notes

1. Argese, M.; Brocchetta, M.; De Miranda, M.; Paoli, P.; Perego, F.; Rossi, P. *Tetrahedron* **2006**, *62*, 6855–6861.
2. Argese, M.; Brocchetta, M.; Manfredi, G.; Rebasti, F.; Ripa, G. WO 01/79207, 2001.
3. Hervè, G.; Bernard, H.; Toupet, L.; Handel, H. *Eur. J. Org. Chem.* **2000**, 33–35.
4. Although theoretical calculations appearing in the lit.[5] and confirmed by those reported in the present article, anticipated that **10** was 'perfectly feasible', it still remained a 'challenging synthetic target' until the trans isomers **6** and **8** were obtained and proved valuable starting materials for its preparation. After **9** and **10** were isolated and characterized, we revised some alkylations performed in the past with ethanes bearing two leaving groups in the 1,2 positions on mixtures containing **1**–**4**.[6] The analysis of the GC chromatograms, acquired with the same method (see Section 4) able to separate **9** and **10**, showed that, apart from **9**, small percentages of a peak with the same retention time of **10** was evidenced. Obviously, a MS–GC study should be undertaken to confirm the presence of **10**.
5. Galasso, V.; Chuburu, F.; Handel, H.; le Baccon, M.; Jones, D. *THEOCHEM* **2002**, *582*, 187–193.
6. Argese, M.; Ripa, G.; Scala, A.; Valle, V. WO 97/49691, 1997.
7. Trademark for sodium dihydrobis(2-methoxyethoxy)aluminate. The compound is largely used for industrial purposes because of the strong reducing power that makes it similar to $LiAlH_4$ but without the drawbacks of the latter, such as pyrophoric nature, short shelf life and limited solubility.
8. Buevich, A.; Chan, T.-M.; Wang, C. H.; McPhail, A. T.; Ganguly, H. K. *Magn. Reson. Chem.* **2005**, *43*, 187–199.
9. (a) Karplus, M. *J. Am. Chem. Soc.* **1963**, *85*, 2870–2871; (b) Jardetzky, C. D. *J. Am. Chem. Soc.* **1961**, *83*, 2919–2920.
10. Desiraju, G. R.; Steiner, T. *The Weak Hydrogen Bond, IUCr Monographs on Crystallography*; Oxford Science Publications: New York, NY, 1999.
11. Crystal data of compounds containing the TAD core were retrieved from the Cambridge Structural Database (CSD, v. 5.27).[12] Only the non-ionic molecules having three-coordinated nitrogens were considered. Among the nine retrieved structures, two are trans-fused and seven have cis-fused rings. In eight of these structures the *d*1 distance is longer than the *d*2 one.
12. Allen, F. H. *Acta Crystallogr.* **2002**, *B58*, 380–388.
13. Cuevas, G.; Juaristi, E. *J. Am. Chem. Soc.* **2002**, *124*, 13088–13096.
14. Hervè, G.; Bernard, H.; Le Bris, N.; Yaouanc, J. J.; Handel, H.; Toupet, L. *Tetrahedron Lett.* **1998**, *39*, 6861–6864.
15. Müller, R.; von Philipsborn, W.; Schleifer, L.; Aped, P.; Fuchs, B. *Tetrahedron* **1991**, *47*, 1013–1036.
16. Sanger, I.; Lerner, H.-W.; Bolte, M. *Acta Crystallogr., Sect. E* **2004**, *60*, 1847–1848.
17. In a previous article,[18] the mp 91–92 °C was reported for a decahydro-2a,4a,6a,8a-tetraazacyclopent[*fg*]acenaphthylene to which the trans stereochemistry was tentatively assigned as the compound was synthesized from *trans* 1,4,5,8-tetraazadecalin under conditions, which should not have induced epimerization. Our data disagree, as they attribute such mp to the cis isomer and mp 136–139 °C to the trans isomer.
18. Ferrari, M.; Giovenzana, G. B.; Palmisano, G.; Sisti, M. *Synth. Commun.* **2000**, *30*, 15–21.
19. The ratio between the cis and trans isomers, which was 1.8/1 in the starting material, became 2.5/1 after the reduction because in the mixtures containing **5**–**8** isomerization phenomena induced by the alkaline pH occur, which favour the increase of the cis compounds.[1]
20. Calculated on the mol (0.0126) of **6** and **8**, which can theoretically afford **10**.
21. *CrysAlis CCD*, Oxford Diffraction: Version 1.171.pre23-10 beta (release 21.06.2004 CrysAlis171.NET) (compiled June 21 2004,12:00:08), Abingdon, Oxfordshire, England.
22. *CrysAlis RED*, Oxford Diffraction: Version 1.171.pre23-10 beta (release 21.06.2004 CrysAlis171.NET) (compiled June 21 2004,12:00:08), Abingdon, Oxfordshire, England.
23. Altomare, A.; Cascarano, G. L.; Giacovazzo, C.; Guagliardi, A.; Burla, M. C.; Polidori, G.; Camalli, M. *J. Appl. Crystallogr.* **1999**, *32*, 115–119.
24. Sheldrick, G. M. *SHELX 97*; University of Göttingen: Göttingen, Germany, 1997.
25. Nardelli, M. *J. Appl. Crystallogr.* **1995**, *28*, 659.
26. Farrugia, L. J. *J. Appl. Crystallogr.* **1997**, *30*, 565.
27. Rojas-Lima, S.; Farfan, N.; Santillan, R.; Castillo, D.; Sosa-Torres, M. E.; Hopfl, M. *Tetrahedron* **2000**, *56*, 6427–6433.
28. Biosym/MSI, San Diego, CA.
29. Chang, G.; Guida, W. C.; Still, W. C. *J. Am. Chem. Soc.* **1989**, *111*, 4379–4386.
30. *Maestro*; Schrodinger: Portland, OR, 2005.
31. (a) Kollman, P. A.; Weiner, S. J.; Case, D. A.; Singh, C.; Ghio, C.; Alagona, G.; Profeta, S.; Weiner, P. *J. Am. Chem. Soc.* **1984**, *106*, 765–784; (b) Weiner, S.; Kollman, P. A. *J. Comput. Chem.* **1986**, *7*, 230–252.
32. Still, W. C.; Tempczyk, A.; Hawley, R. C.; Hendrickson, T. *J. Am. Chem. Soc.* **1990**, *112*, 6127–6129.
33. Ponder, J. W.; Richards, F. M. *J. Comput. Chem.* **1987**, *8*, 1016–1024.
34. Frisch, M. J.; Trucks, G. W.; Schlegel, H. B.; Scuseria, G. E.; Robb, M. A.; Cheeseman, J. R.; Montgomery, J. A., Jr.; Vreven, T.; Kudin, K. N.; Burant, J. C.; Millam, J. M.; Iyengar, S. S.; Tomasi, J.; Barone, V.; Mennucci, B.; Cossi, M.; Scalmani, G.; Rega, N.; Petersson, G. A.; Nakatsuji, H.; Hada, M.; Ehara, M.; Toyota, K.; Fukuda, R.; Hasegawa, J.; Ishida, M.; Nakajima, T.; Honda, Y.; Kitao, O.; Nakai, H.; Klene, M.; Li, X.; Knox, J. E.; Hratchian, H. P.; Cross, J. B.; Adamo, C.; Jaramillo, J.; Gomperts, R.; Stratmann, R. E.; Yazyev, O.; Austin, A. J.; Cammi, R.; Pomelli, C.; Ochterski, J. W.; Ayala, P. Y.; Morokuma, K.; Voth, G. A.; Salvador, P.; Dannenberg, J. J.; Zakrzewski, V. G.; Dapprich, S.; Daniels, A. D.; Strain, M. C.; Farkas, O.; Malick, D. K.; Rabuck, A. D.; Raghavachari, K.; Foresman, J. B.; Ortiz, J. V.; Cui, Q.; Baboul, A. G.; Clifford, S.; Cioslowski, J.; Stefanov,

B. B.; Liu, G.; Liashenko, A.; Piskorz, P.; Komaromi, I.; Martin, R. L.; Fox, D. J.; Keith, T.; Al-Laham, M. A.; Peng, C. Y.; Nanayakkara, A.; Challacombe, M.; Gill, P. M. W.; Johnson, B.; Chen, W.; Wong, M. W.; Gonzalez, C.; Pople, J. A. *Gaussian 03, Revision B05*; Gaussian: Pittsburgh, PA, 2003.
35. Gordon, M. S. *Chem. Phys. Lett.* **1980**, *76*, 163–168.
36. Peng, C.; Ayala, P. Y.; Schlegel, H. B.; Frisch, M. J. *J. Comput. Chem.* **1996**, *17*, 49–56.
37. Frisch, M. J.; Head-Gordon, M.; Pople, J. A. *Chem. Phys. Lett.* **1990**, *166*, 281–289.
38. Glendening, E. D.; Badenhoop, J. K.; Reed, A. E.; Carpenter, J. E.; Bohmann, J. A.; Morales, C. M.; Weinhold, F. *NBO 5.0*; Theoretical Chemical Institute, University of Wisconsin: Madison, WI, 2001.
39. *Spartan'02*; Wavefunction: Irvine, CA, 2002.
40. Becke, A. D. *J. Chem. Phys.* **1993**, *98*, 5648–5652.
41. Lee, C.; Yang, W.; Parr, R. G. *Phys. Rev. B* **1998**, *37*, 785–789.